PROCEEDINGS OF SCIENCE

Probing neutrino interactions and properties with IceCube

Mohamed Rameez[a,*] **for the IceCube Collaboration**[*]

[a] *Department of High Energy Physics,*
Tata Institute of Fundamental Research
Homi Bhabha Road, Colaba,
Mumbai - 400005, Maharashtra, India

E-mail: mohamed.rameez@tifr.res.in

Instrumenting a cubic kilometre of ice at the South Pole, the IceCube neutrino observatory has confirmed the existence of a diffuse flux of astrophysical neutrinos at TeV-PeV energies, opening a new window to the cosmos. This flux, along with that of neutrinos produced in interactions of cosmic rays in the upper atmosphere, enable the study of neutrino interactions at energies far beyond that which is achievable with beams produced on Earth. The Glashow resonance, an on-shell production of the W^- boson due to the interaction of a $\bar{\nu}_e$ of ~ 6.3 PeV with an electron has been confirmed at ~100:1 odds, while the cross section with which neutrinos interact with nucleons at TeV-PeV energies, as well as the distribution of inelasticity in these interactions have been found to be compatible with Standard Model expectations. The observed zenith dependent deficit in the number of ν_μ (and $\bar{\nu}_\mu$) interacting and contained within the detector at GeV energies has provided measurements of the neutrino oscillation parameters $|\Delta m^2_{32}|$ and $\sin^2(\theta_{23})$ at precisions comparable to that of terrestrial accelerator based neutrino beam experiments. The flavour ratio of the astrophysical neutrino flux provides the most stringent probe so far for quantum-gravity-motivated physics. The next great leap in the study of fundamental physics with cosmic neutrinos requires the construction of IceCube-Gen2, ten times larger and extending the sensitivity to EeV energies.

16th International Conference on Heavy Quarks and Leptons (HQL2023)
28 November-2 December 2023
TIFR, Mumbai, Maharashtra, India

[*] https://authorlist.icecube.wisc.edu/icecube
[*] Speaker

PoS(HQL2023)028

1. Introduction

IceCube is a cubic kilometer sized neutrino detector [1], deployed at the South Pole between 2004 and 2010. The optical array consists of 5160 Digital Optical Modules (DOMs) - each built around a photomultiplier tube, embedded in the ice along 86 vertical strings at depths between 1450 m and 2450 m. The DOMs detect Cherenkov photons emitted by relativistic charged particles in the ice. Typical events observed by IceCube can be classified broadly into two topologies. Muons traversing the ice leave a long track-like pattern of hits within the detector, while electromagnetic and hadronic showers appear as almost spherical blobs of hits known as cascades. When the track is due to a muon which originates in the charged current interaction of a ν_μ (or $\bar{\nu}_\mu$), the direction of the incoming neutrino can be inferred to less than 1° precision. Cascades on the other hand require accurate modelling of the propagation of photons in ice in order to be reconstructed. This has been steadily improving and angular resolutions as good as 7° have been achieved [2]. Cascades however allow the energy of the primary neutrino to be inferred to within $\sim$ 30% precision, while tracks most often allow only a lower limit on the energy of the primary to be obtained, as they are not necessarily contained within the instrumented region of the ice.

The principal IceCube array is able to reconstruct events originating in the interactions of neutrinos above $\sim$ 100 GeV, while the more densely instrumented DeepCore region at the deep central part of the detector lowers this threshold to $\sim$ 10 GeV.

In 2013, IceCube confirmed the existence of a diffuse neutrino flux of astrophysical origin [3] at TeV-PeV energies. These measurements were done using the High Energy Starting Event (HESE) sample [4] which employed the outermost layer of the detector as a veto and selected only events above ~60 TeV in order to suppress the background of atmospheric neutrinos and muons.

Subsequently, candidate sources have been identified for the astrophysical flux, partly due to the advent of real-time multimessenger astronomy [5–7]. A diffuse component coming from the plane of our own Galaxy has also been identified [2].

These discoveries mark the grand-triumph of IceCube, as a tool for astronomy with neutrinos, opening a new window to the Universe and forever changing mankind's perception of it. They have also opened up avenues to study neutrino interactions at energies far beyond the reach of beams that can be produced on Earth. In this manuscript we briefly report on a select few insights from these studies.

2. Detection of a particle shower at the Glashow resonance

Neutrinos are fundamental particles which couple to matter only via the exchange of W and Z bosons. It was predicted back in 1960 that in the interaction of $\bar{\nu}_e$ with electrons, the cross section would be resonantly enhanced due to the s-channel, on shell production of a W^- boson [8] at a center of mass energy corresponding to the mass of the W boson. When the mass of the W boson was eventually measured, the neutrino energy required in the rest frame of the electron for this Glashow resonance was predicted to be 6.32 PeV, beyond the reach of terrestrial accelerators.

On 8th December 2016, IceCube detected an event with a visible energy of 6.05 ± 0.72 PeV [9]. Its energy and direction determined it to be of astrophysical origin at $> 5\sigma$. The DOMs closest to the reconstructed interaction point of the event detected photons earlier than would be expected from a purely electromagnetic shower (see Figure 1). Taking into account the energy resolution of the detector, the relative cross sections of the Glashow resonance w.r.t. that of off resonance deep inelastic scattering favour this event to be from the hadronic decay of a resonantly produced W^- boson at 100:1 odds (see Figure 3 of [9]), assuming the best fit astrophysical neutrino flux from a combined analysis of various IceCube datasets.

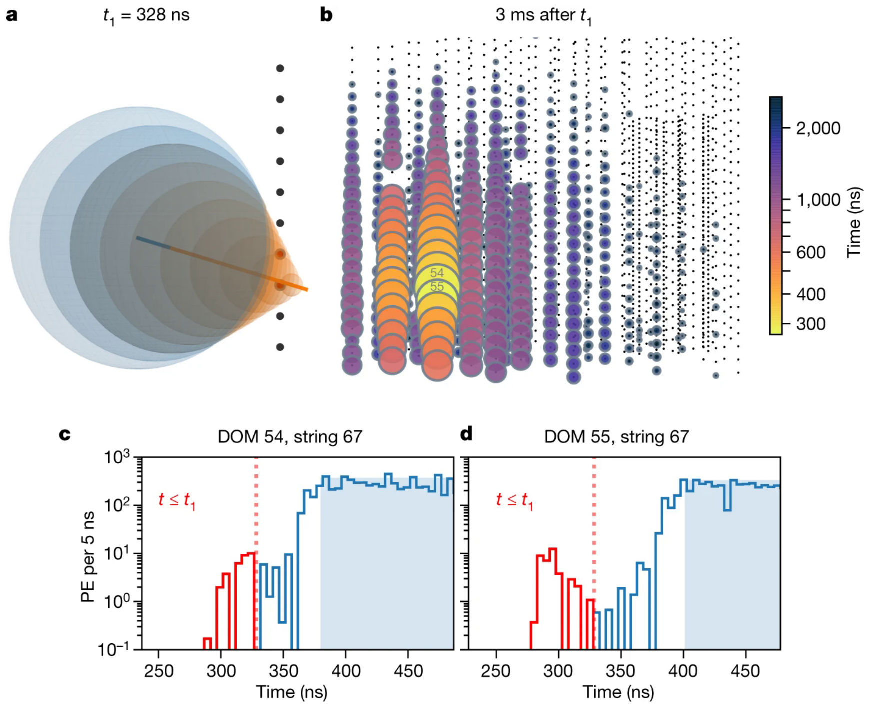

Figure 1: Photons detected at different times in the Glashow resonance event. a, Schematic of an escaping muon travelling faster than light (in ice) and its Cherenkov cone (orange). The muons reach the nearest modules ahead of the Cherenkov photons produced by the EM component of the hadronic shower (blue) as these travel at the speed of light in ice. The blue part of the line is the main shower, while the orange line is associated with the muons. Each black dot arranged vertically is a DOM on the nearest string, with the two (slightly larger) dots inside the orange cone the first two to observe early pulses. The time t_1 indicates the approximate time elapsed since the neutrino interaction at which this snapshot graphic was taken. **b**, Event view, showing DOMs that triggered across IceCube at a later time. Each bubble represents a DOM, with its size proportional to the detected charge. Colours indicate the time of first trigger for each DOM, relative to the best fit time of the initial interaction. The small black dots are DOMs further away with no detected photons within 3 ms of t_1. **c, d,** Distributions of the deposited charge over time on the two earliest hit DOMs. The dotted red line is at $t_1 = 328ns$, the instant shown in **a**. The histogram in red (blue) shows photons arriving before (after) t_1, and the blue shaded region denotes saturation of the photomultiplier tube. For more details see ref. [2] from where this figure has been taken.

3. Measurement of the neutrino-nucleon cross section at TeV energies

At energies above 40 TeV, the Earth starts becoming opaque to neutrinos. This leads to a suppression of the neutrino flux arriving at IceCube w.r.t. that at the Earth's surface, depending upon the energy as well as the column density of the Earth along the line of sight. By comparing the observed zenith distribution of data in the HESE sample with theoretical expectations (see Figure 2), the charged current all flavour neutrino cross section was measured in four energy bins between 60 TeV and 10 PeV [10]. The results were found to be compatible with Standard Model expectations, and thus constrain scenarios which predict a steep rise in the cross section above ~ 1 PeV due to the existence of new exotic particles such as lepto-quarks or sphalerons.

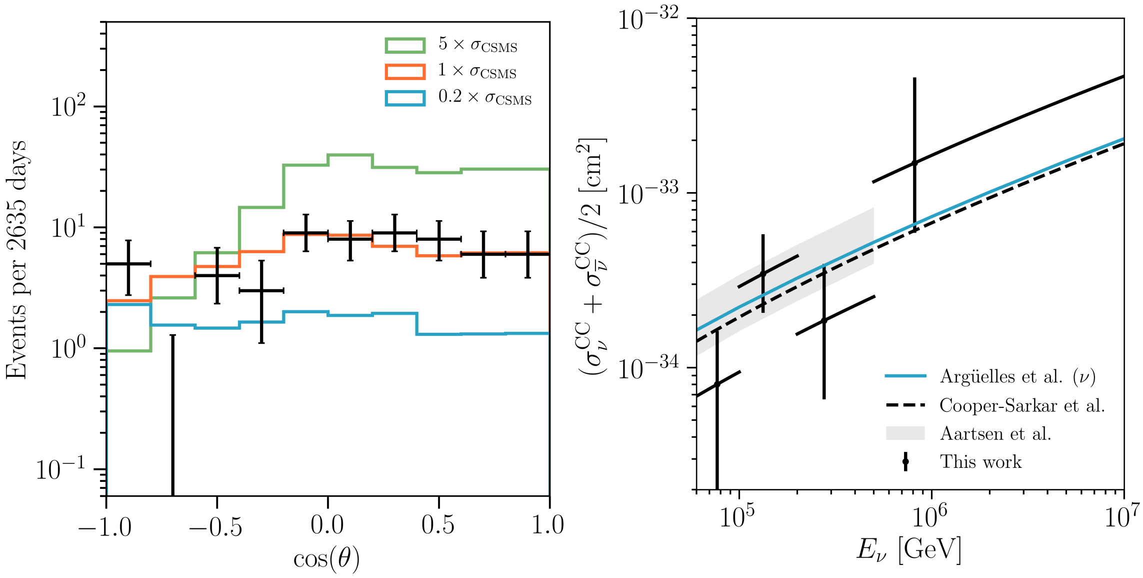

Figure 2: Left: The zenith distribution of data and the best-fit, single-power-law flux expectation assuming σ_{CSMS} (orange) [11]. Predictions from two other cross sections are also shown, assuming the same flux. The effect of rescaling the cross section is linear in the southern sky, $\cos\theta > 0$, due to the Earth absorption being negligible. In the northern sky, $\cos\theta < 0$, the strength of Earth absorption depends on the cross section, as well as the neutrino energy and zenith angle. Right: The charged-current, high-energy neutrino cross section as a function of energy, averaged over ν and $\bar{\nu}$. The Wilks' 1-sigma CI is shown along with two cross section calculations [11, 12]. The confidence intervals from an earlier measurement [13] are also shown for comparison. Figures taken from ref. [10].

4. Measurements with the inelasticity distribution

The fraction of the energy of the incoming neutrino which is transferred to hadrons in a deep inelastic collision is known as the inelasticity, y. In a sample of contained neutrino interactions isolated from 5 years of IceCube data (2650 tracks and 965 cascades) the mean inelasticity ⟨y⟩ was measured in 5 bins in the range of 3.5 TeV to 2.6 PeV, and were found to be consistent with Standard Model predictions (see Figure 3) [14]. The expected difference in the y distributions between ν_μ and $\bar{\nu}_\mu$ interactions was exploited to measure the ratio of ν_μ to $\bar{\nu}_\mu$ in the atmospheric neutrino flux between 770 GeV and 21 TeV to be $0.77^{+0.44}_{-0.25}$ times the HKKMS[15] prediction. Since the production of charmed mesons in neutrino charged current interactions is expected to modify the y distributions, the data has been used to exclude the zero charm production scenario at 91% confidence level, and are compatible with a leading order estimate of charm production.

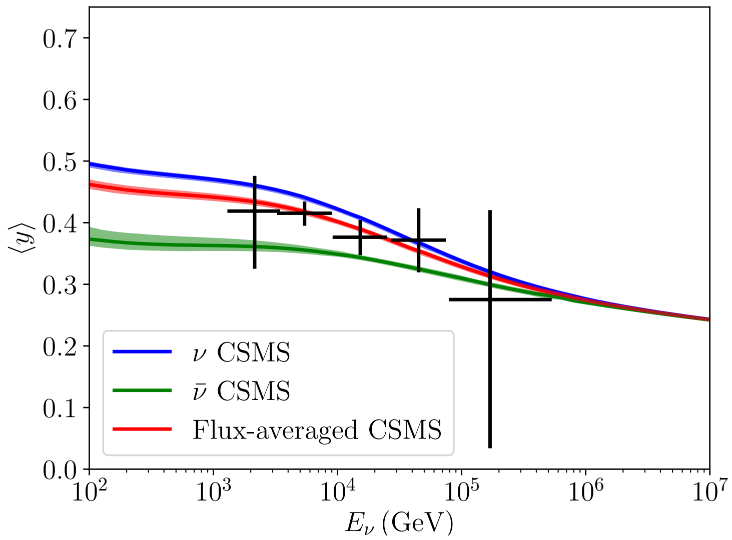

Figure 3: The measured mean inelasticity in five bins of reconstructed energy. Vertical error bars indicate the 68% confidence interval for the mean inelasticity, and horizontal error bars indicate the expected central 68% of neutrino energies in each bin. The predicted mean inelasticity from CSMS [11] is shown in blue for neutrinos and in green for antineutrinos. The height of the colored bands indicates theoretical uncertainties in the CSMS calculation. A flux-averaged mean inelasticity according to the HKKMS [15] calculation is shown in red. Figure taken from ref. [14].

5. Neutrino oscillations

Incontrovertible evidence has emerged over the last few decades for the fact that neutrinos are massive particles. The phenomenon of neutrino oscillations paints a picture in which neutrinos are produced in their flavour eigenstates while they propagate as their mass eigenstates. Because the mass eigenstates interfere during propagation, the probability that a neutrino which was produced in one flavour eigenstate is observed in another depends periodically on the square of the mass difference Δm^2 as well as the ratio of the distance of propagation L to the neutrino energy E. For atmospheric neutrinos detected by IceCube, L is specified by the arrival direction of the neutrino.

By measuring the relative flux of neutrino flavours as a function of their reconstructed energies and arrival directions using a data sample of IceCube-DeepCore recorded between 2011-2019 [17], IceCube has been able to constrain the neutrino mixing parameters Δm^2_{32} and $\sin^2(\theta_{23})$ (see Figure 4). This is the most precise measurement of neutrino oscillation parameters using atmospheric neutrinos, improving upon previous results[16] in terms of data calibration, detector simulation and data processing. It is competitive with measurements performed with man made neutrino beams.

By performing a similar analysis of events between 320 GeV and 20 TeV, IceCube has also been able to place stringent constraints on the parameter space of sterile neutrinos [22], excluding the region favoured by the LSND and MiniBooNe anomaly at more than 99% Confidence Level.

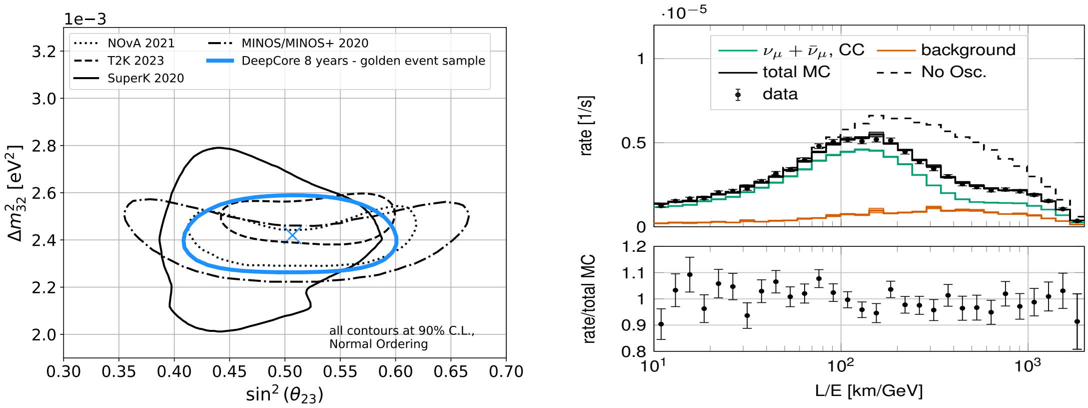

Figure 4: Left : Contours showing the 90% C.L. allowed region for the atmospheric neutrino oscillation parameters from this study (blue) compared to results from MINOS [18], NOvA [19], Super-Kamiokande [20] and T2K [21]. The DeepCore confidence interval is derived assuming Wilks' theorem. Right : The L/E distribution for the best-fit expectations overlaid with the observed data. Background includes atmospheric μ and all neutrino types besides $\nu_\mu + \bar{\nu}_\mu$ CC events. The expectation at the best fit but without oscillations is shown as a dashed line. Figures taken from ref. [17].

6. Constraints on Quantum Gravity from the flavour ratio of astrophysical neutrinos

Astrophysical neutrinos propagate unperturbed over billions of light years in the vacuum of space. Effects of Quantum Gravity, while considered too weak to be observable today in kinematics due to their suppression by the Planck Energy E_p or its higher powers, nevertheless can cause observable flavour conversions through the phase shift of neutrino waves accumulated over astrophysical baselines. The observed flavour ratio of the 7.5 year HESE sample of events (see Figure 5) provides the most stringent constraints on the Wilson coefficients of the dimension 6 operators which parameterize new space-time structure due to Quantum Gravity effects, reaching down to 10^{-42} GeV^{-2} for specific astrophysical production scenarios (Figure 6). While these assumed specific production scenarios are to be tested using multimessenger studies of astrophysical neutrino sources, the constraints are below what is expected to be 'natural' at E_p^{-2} ($\sim 10^{-38}$ GeV^{-2}), exemplifying neutrino astronomy and the multimessenger study of neutrino sources as the most promising probe of Quantum Gravity effects in the foreseeable future [23].

7. The Future

The aforementioned results are but a small sample of the ways in which astroparticle physics experiments, in particular neutrino telescopes can be used to study phenomena similar to those which are probed at particle colliders, by utilizing fluxes of high energy particles provided to us by the cosmos, instead of expending vast quantities of energy accelerating them. By looking for an excess of neutrinos from the directions of astrophysical objects which are dominated by Dark Matter [27], or objects in which Dark Matter can get gravitationally captured [28], IceCube is able to place stringent bounds on the cross sections with which Dark Matter interacts with ordinary

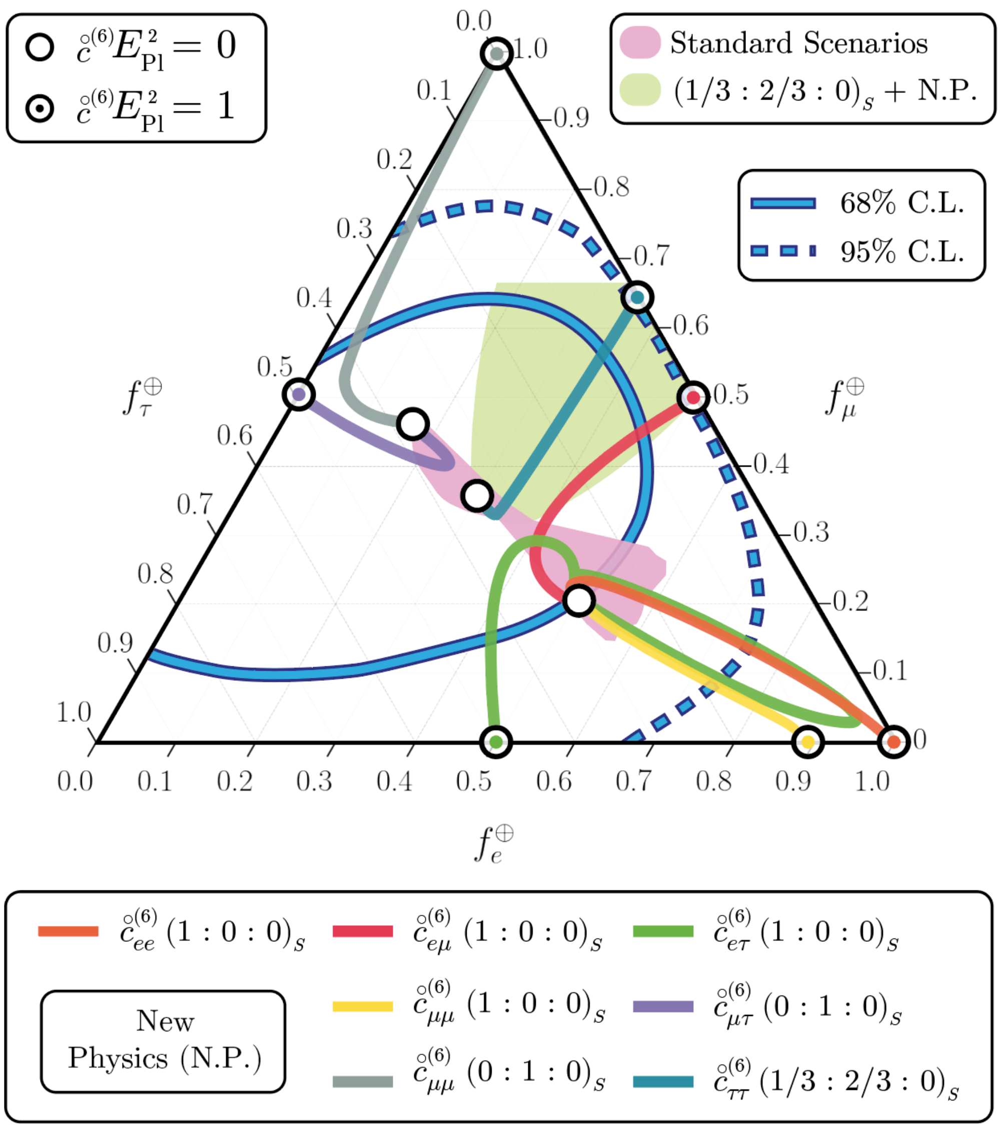

Figure 5: ***Flavour triangle of the Astrophysical neutrino flux, including illustrations of new physics effects and contours from data.*** The figure represents the flavour ratio ($\nu_e : \nu_\mu : \nu_\tau$) of specific compositions at the source (S); the corners indicate pure ν_e, ν_μ, or ν_τ composition. The blue solid and dashed lines correspond to 68% and 95% C.L. contours [24] from IceCube data respectively. The pink region represents expected flavour ratios from the standard astrophysical neutrino production models, where the neutrinos at the production source are all possible combinations of ν_e and ν_μ with the neutrino oscillation parameter uncertainties obtained in [25]. The lines explained in the lower legend illustrate the effects of the new physics (NP) operators. Three astrophysical neutrino production models are highlighted by ○ symbols, a ν_μ dominant source (0:1:0)$_S$ (top), a ν_e dominant source (1:0:0)$_S$ (bottom), and a preferred model (1/3:2/3:0)$_S$ (middle). When new physics operators are small ($\leq m^2/2E$), they are distributed within the central region. If the values of NP operators are increased, predicted flavour ratios start to move away from the centre, and they reach to ⊙ symbols when the NP effects are large ($\sim E_P^{-2}$). For simplicity this analysis focussed on real, positive new physics potentials. Figure taken from ref. [23].

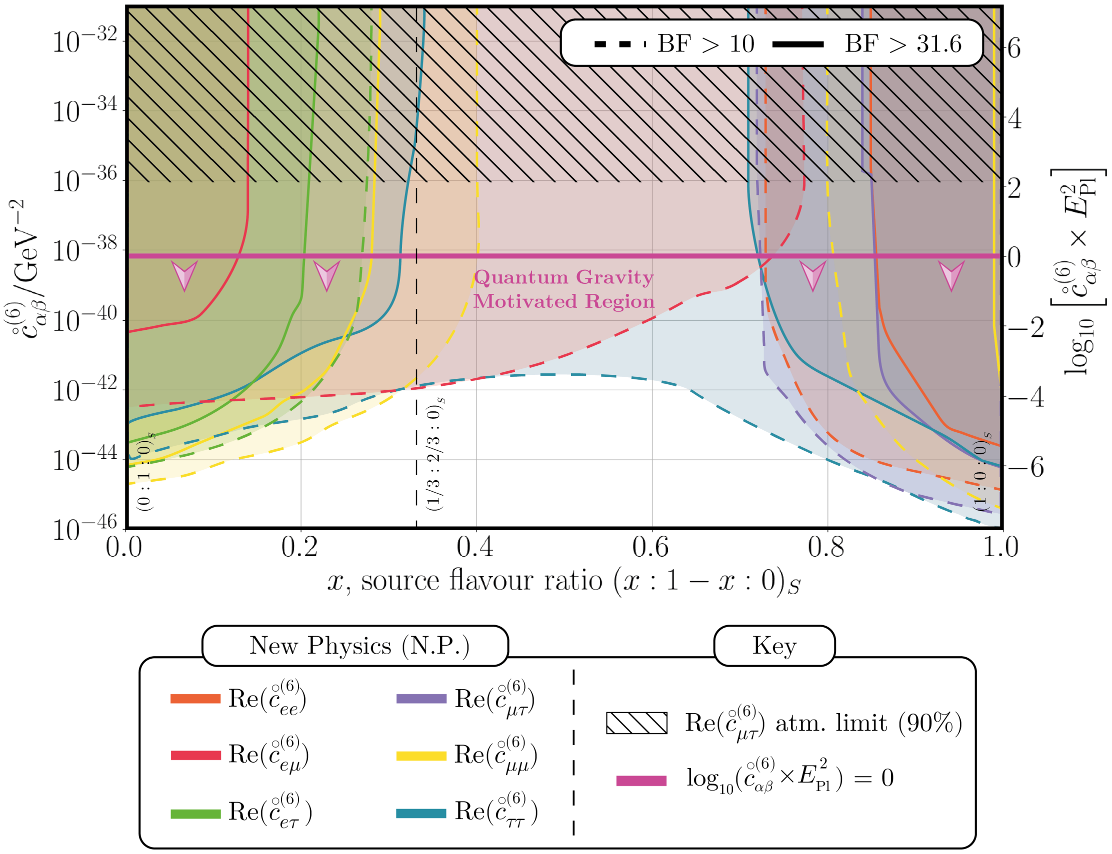

Figure 6: ***Limits on the dimension-six new physics operators.*** The hatched region shows the limit obtained from the atmospheric neutrino data analysis [26]. Limits are presented as a function of the assumed astrophysical neutrino flavour ratio at the production source. The leftmost scenario is ν_μ dominant $(0{:}1{:}0)_S$ and the rightmost is ν_e dominant $(1{:}0{:}0)_S$ The preferred scenario corresponds to $(1/3{:}2/3{:}0)_S$ (dashed vertical line). For more details see ref. [23]. Figure taken from ref. [23].

matter, or annihilates with itself. In the parameter spaces of minimal extensions of the Standard Model conjured up to solve the Dark Matter puzzle, these constraints are complementary to those from colliders [29] and direct detection experiments [30].

While the astroparticle context suffers from an inability to perform repeatable experiments - a key strength of the collider programme, it nevertheless provides powerful consistency tests of our reductionist descriptions of phenomena at the highest energy scales, in addition to their primary purpose of studying the Universe using high energy particles. As we stand in 2024, confronted with the myriad choices of how to deploy limited economic resources to further our understanding of fundamental physics, neutrino telescopes mark themselves out to be an attractive option, promising a hint of the same kind of physics pursued by the effort to build ever larger colliders.

The proposed IceCube-Gen2 [31] extension to IceCube will instrument 10 times the volume of ice, increasing the rate of astrophysical neutrinos by a factor of ~ 10, allowing sources five times fainter to be detected[1]. A radio array will further extend the sensitivity to EeV energies.

References

[1] M. G. Aartsen *et al.* [IceCube], JINST **12** (2017) no.03, P03012 doi:10.1088/1748-0221/12/03/P03012 [arXiv:1612.05093 [astro-ph.IM]].

[2] R. Abbasi *et al.* [IceCube], Science **380** (2023) no.6652, adc9818 doi:10.1126/science.adc9818 [arXiv:2307.04427 [astro-ph.HE]].

[3] M. G. Aartsen *et al.* [IceCube], Science **342** (2013), 1242856 doi:10.1126/science.1242856 [arXiv:1311.5238 [astro-ph.HE]].

[4] R. Abbasi *et al.* [IceCube], Phys. Rev. D **104** (2021), 022002 doi:10.1103/PhysRevD.104.022002 [arXiv:2011.03545 [astro-ph.HE]].

[5] M. G. Aartsen *et al.* [IceCube, Fermi-LAT, MAGIC, AGILE, ASAS-SN, HAWC, H.E.S.S., INTEGRAL, Kanata, Kiso, Kapteyn, Liverpool Telescope, Subaru, Swift NuSTAR, VERITAS and VLA/17B-403], Science **361** (2018) no.6398, eaat1378 doi:10.1126/science.aat1378 [arXiv:1807.08816 [astro-ph.HE]].

[6] M. G. Aartsen *et al.* [IceCube], Science **361** (2018) no.6398, 147-151 doi:10.1126/science.aat2890 [arXiv:1807.08794 [astro-ph.HE]].

[7] R. Abbasi *et al.* [IceCube], Science **378** (2022) no.6619, 538-543 doi:10.1126/science.abg3395 [arXiv:2211.09972 [astro-ph.HE]].

[8] S. L. Glashow, Phys. Rev. **118** (1960), 316-317 doi:10.1103/PhysRev.118.316

[9] M. G. Aartsen *et al.* [IceCube], Nature **591** (2021) no.7849, 220-224 [erratum: Nature **592** (2021) no.7855, E11] doi:10.1038/s41586-021-03256-1 [arXiv:2110.15051 [hep-ex]].

[10] R. Abbasi *et al.* [IceCube], doi:10.1103/PhysRevD.104.022001 [arXiv:2011.03560 [hep-ex]].

[11] A. Cooper-Sarkar, P. Mertsch and S. Sarkar, JHEP **08** (2011), 042 doi:10.1007/JHEP08(2011)042 [arXiv:1106.3723 [hep-ph]].

[12] C. A. Argüelles, F. Halzen, L. Wille, M. Kroll and M. H. Reno, Phys. Rev. D **92** (2015) no.7, 074040 doi:10.1103/PhysRevD.92.074040 [arXiv:1504.06639 [hep-ph]].

[13] M. G. Aartsen *et al.* [IceCube], Nature **551**, 596-600 (2017) doi:10.1038/nature24459 [arXiv:1711.08119 [hep-ex]].

[14] M. G. Aartsen *et al.* [IceCube], Phys. Rev. D **99** (2019) no.3, 032004 doi:10.1103/PhysRevD.99.032004 [arXiv:1808.07629 [hep-ex]].

[15] M. Honda, T. Kajita, K. Kasahara, S. Midorikawa and T. Sanuki, Phys. Rev. D **75** (2007), 043006 doi:10.1103/PhysRevD.75.043006 [arXiv:astro-ph/0611418 [astro-ph]].

[1] https://icecube-gen2.wisc.edu/science/publications/TDR/

[16] M. G. Aartsen *et al.* [IceCube], Phys. Rev. Lett. **120** (2018) no.7, 071801 doi:10.1103/PhysRevLett.120.071801 [arXiv:1707.07081 [hep-ex]].

[17] R. Abbasi *et al.* [(IceCube Collaboration)* and IceCube], Phys. Rev. D **108** (2023) no.1, 012014 doi:10.1103/PhysRevD.108.012014 [arXiv:2304.12236 [hep-ex]].

[18] P. Adamson *et al.* [MINOS+], Phys. Rev. Lett. **125** (2020) no.13, 131802 doi:10.1103/PhysRevLett.125.131802 [arXiv:2006.15208 [hep-ex]].

[19] M. A. Acero *et al.* [NOvA], Phys. Rev. D **106** (2022) no.3, 032004 doi:10.1103/PhysRevD.106.032004 [arXiv:2108.08219 [hep-ex]].

[20] P. Fernandez Menendez [Super-Kamiokande], PoS **ICRC2021** (2021), 008 doi:10.22323/1.395.0008

[21] K. Abe *et al.* [T2K], Eur. Phys. J. C **83** (2023) no.9, 782 doi:10.1140/epjc/s10052-023-11819-x [arXiv:2303.03222 [hep-ex]].

[22] M. G. Aartsen *et al.* [IceCube], Phys. Rev. Lett. **117** (2016) no.7, 071801 doi:10.1103/PhysRevLett.117.071801 [arXiv:1605.01990 [hep-ex]].

[23] R. Abbasi *et al.* [IceCube], Nature Phys. **18** (2022) no.11, 1287-1292 doi:10.1038/s41567-022-01762-1 [arXiv:2111.04654 [hep-ex]].

[24] R. Abbasi *et al.* [IceCube], Eur. Phys. J. C **82** (2022) no.11, 1031 doi:10.1140/epjc/s10052-022-10795-y [arXiv:2011.03561 [hep-ex]].

[25] I. Esteban, M. C. Gonzalez-Garcia, M. Maltoni, T. Schwetz and A. Zhou, JHEP **09** (2020), 178 doi:10.1007/JHEP09(2020)178 [arXiv:2007.14792 [hep-ph]].

[26] M. G. Aartsen *et al.* [IceCube], Nature Phys. **14** (2018) no.9, 961-966 doi:10.1038/s41567-018-0172-2 [arXiv:1709.03434 [hep-ex]].

[27] M. G. Aartsen *et al.* [IceCube], Eur. Phys. J. C **77** (2017) no.9, 627 doi:10.1140/epjc/s10052-017-5213-y [arXiv:1705.08103 [hep-ex]].

[28] M. G. Aartsen *et al.* [IceCube], Eur. Phys. J. C **77** (2017) no.3, 146 [erratum: Eur. Phys. J. C **79** (2019) no.3, 214] doi:10.1140/epjc/s10052-017-4689-9 [arXiv:1612.05949 [astro-ph.HE]].

[29] T. Jacques, A. Katz, E. Morgante, D. Racco, M. Rameez and A. Riotto, JHEP **10** (2016), 071 [erratum: JHEP **01** (2019), 127] doi:10.1007/JHEP10(2016)071 [arXiv:1605.06513 [hep-ph]].

[30] M. G. Aartsen *et al.* [IceCube and PICO], Eur. Phys. J. C **80** (2020) no.9, 819 doi:10.1140/epjc/s10052-020-8069-5 [arXiv:1907.12509 [astro-ph.HE]].

[31] M. G. Aartsen *et al.* [IceCube-Gen2], J. Phys. G **48** (2021) no.6, 060501 doi:10.1088/1361-6471/abbd48 [arXiv:2008.04323 [astro-ph.HE]].